http://dx.doi.org/10.5012/bkcs.2012.33.10.3489

Facile Synthesis of $BaWO_4$ Sub-Micron Sized Octahedron *via* a Microemulsion Method

Kun Kim and Young-Duk Huh*

Department of Chemistry, Institute of Nanosensor and Biotechnology, Dankook University, Gyeonggi-Do 448-701, Korea
**E-mail: ydhuh@dankook.ac.kr*
Received June 13, 2012, Accepted July 19, 2012

Key Words : $BaWO_4$, Microemulsion, Morphology

Morphology-controlled synthesis is one of the important issues in the study of inorganic oxides. A variety of synthetic methods have been used for the preparation of the morphology-controlled inorganic oxides.[1-4] Among these methods, the microemulsion methods have been widely used for the control of the size and morphology of inorganic oxides.[5-7] The unique atomic arrangements on the surfaces can be obtained from the inorganic oxides with specific morphology. The physical properties, such as optical, catalytical, and antibacterial properties, are significantly affected by the surfaces of inorganic oxides.[8-10] The cubic and octahedral morphologies have attracted considerable interest for their specific surfaces. In recently, the photocatalytic activity of octahedral Cu_2O was investigated with comparison of the cubic Cu_2O. The results demonstrate that the photocatalytic activity of octahedral Cu_2O is much higher than that of cubic Cu_2O.[11,12] Therefore, the morphology-controlled synthesis for the cubic and octahedral inorganic oxides is important for investigating their morphology-dependent physical properties.

$BaWO_4$ is an important inorganic oxide used as an electro-optical material and Raman converters. Various morphologies of $BaWO_4$ including cubes, rods, wires, and ribbons have been obtained.[13-16] Most of these works have focused on the preparation of nanosized crystals. However, relatively little is known about the morphology-controlled synthesis of sub-micron sized $BaWO_4$.[17] To investigate the morphology-dependent bulk physical properties excluding a confined effect of nano-sized crystals, sub-micron and micron sized crystals with well-defined morphologies, such as cube and octahedron, have to be prepared. Here we report a simple microemulsion method for the preparation of $BaWO_4$ sub-micron sized octahedra. We also examined the changes of morphology by adjusting the experimental conditions.

Figure 1 shows the typical XRD pattern of the $BaWO_4$ product obtained from the microemulsion method using a cetyltrimethyl ammonium bromide (CTAB)/water/cyclohexane/*n*-butanol quaternary system. All the diffraction peaks corresponded to the tetragonal crystal type of $BaWO_4$ (a = b = 0.561 nm, c = 1.272 nm) and matched very well to the reported data for this system (JCPDS 85-0588). The morphology of $BaWO_4$ products was revealed by identifying their SEM images.

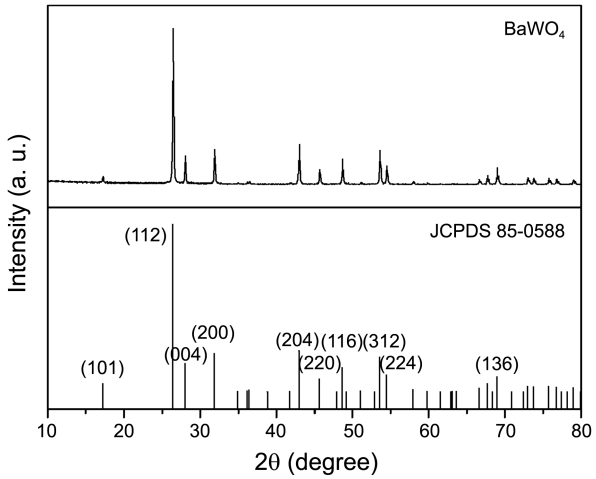

Figure 1. XRD pattern of the $BaWO_4$ product obtained by the microemulsion method of ω = 10 with $[Ba^{2+}] = [WO_4^{2-}]$ at 60 °C for 3 h.

Figure 2 shows the SEM images of $BaWO_4$ products prepared by the microemulsion method at different values of ω (= $[H_2O]/[CTAB]$). At ω = 5, an octahedron of $BaWO_4$ was obtained, as shown in Figure 2(a). The average side length of the octahedron was 100 nm. When ω was increased to 10 by simply decreasing the CTAB amount with other conditions held constant, a larger octahedron of $BaWO_4$ was obtained compared to the that of ω = 5. The average side length of the octahedron was also increased to 150 nm, as shown in Figure 2(b). When the value of ω was further increased to 14, a corner-truncated octahedron with an average side length of approximately 200 nm was observed, as shown in Figure 2(c). When the value of ω was finally increased to 16, a highly corner-truncated octahedron with an average side length of approximately 260 nm was observed, as shown in Figure 2(d). This result indicates that the size of $BaWO_4$ strongly depends on the value of ω. At higher values of ω, a smaller amount of CTAB was used to keep the amount of H_2O constant, and the diameter of the microemulsion droplet was increased to reduce the surface area to the total volume. Therefore, a larger sized octahedron of $BaWO_4$ was formed due to a larger confined volume of larger sized microemulsion droplet at a higher value of ω. Therefore, the results conclusively demonstrate that the size

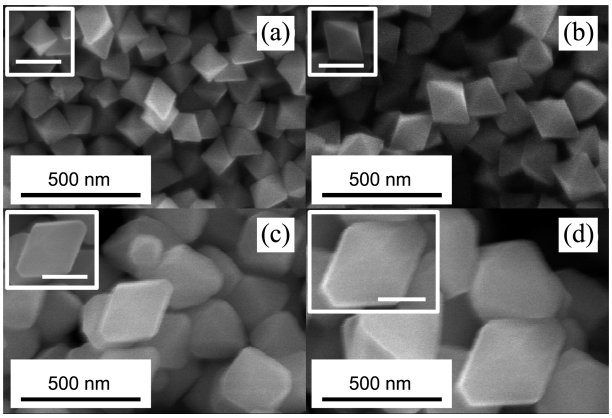

Figure 2. SEM images of $BaWO_4$ products prepared by the microemulsion method with $[Ba^{2+}] = [WO_4^{2-}]$ at 60 °C for 3 h for different values of ω: (a) ω = 5, (b) ω = 10, (c) ω = 14, and (d) ω = 16. The insets show high-magnification SEM images with scale bars of 200 nm.

of the octahedra of $BaWO_4$ products increased with the value of ω. Above ω = 14, a corner-truncated octahedra were obtained and the degree of truncation increased at higher values of ω. When ω was higher than 16, the transparent microemulsion solution could not be obtained, and the microemulsion method could not be applied for the $BaWO_4$ products. Liu and Chu prepared octahedral $BaWO_4$ using a microemulsion-mediated hydrothermal method.[17] The morphology of $BaWO_4$ microparticles strongly depends on the CTAB concentration. At a lower CTAB concentration, spherical $BaWO_4$ nanoparticles were obtained. In a moderate CTAB concentration, octahedral $BaWO_4$ particles with blurred shaped at the edge areas were observed. If the CTAB concentration was further increased, irregular polyhedral $BaWO_4$ particles were obtained. Our results shows more fine morphological tuning of octahedral $BaWO_4$ particles with the values of ω (= $[H_2O]/[CTAB]$) by changing the CTAB concentration with other conditions held constant.

Figure 3(a) shows a transmission electron microscopy (TEM) image of $BaWO_4$ products prepared by the microemulsion method of ω = 10. The octahedra with 150 nm in side length were obtained. Figure 3(b) shows high resolution TEM (HRTEM) images of corner surface of an individual

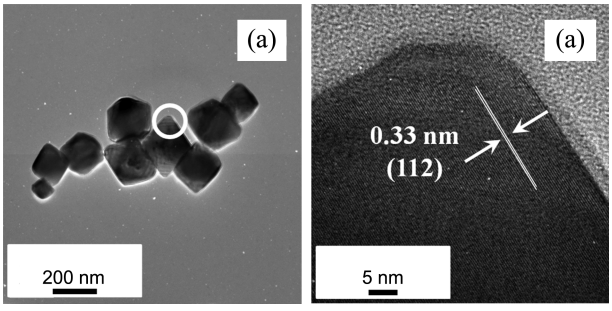

Figure 3. (a) TEM images of $BaWO_4$ products prepared by the microemulsion method of ω = 10 with $[Ba^{2+}] = [WO_4^{2-}]$ at 60 °C for 3 h. (b) HRTEM images of corner surface of an individual $BaWO_4$ octahedron.

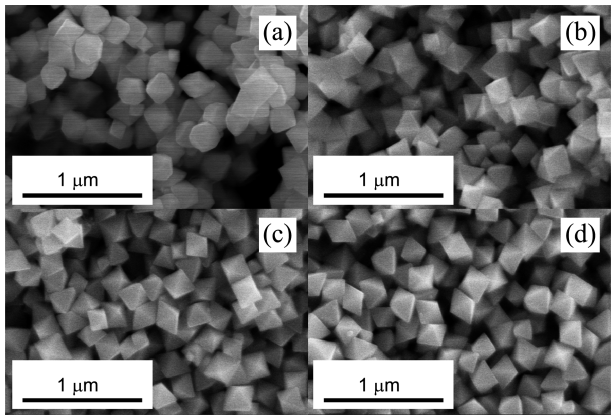

Figure 4. SEM images of $BaWO_4$ products prepared by the microemulsion method of ω = 10 with $[Ba^{2+}] = [WO_4^{2-}]$ at 60 °C for different incubation times: (a) 10 min, (b) 1 h, (c) 3 h, and (d) 6 h.

$BaWO_4$ octahedron. The fringe pattern of the corner surface indicates spacing of 0.33 nm, which corresponds to the (112) plane of a tetragonal $BaWO_4$ crystal. The HRTEM image of individual $BaWO_4$ octahedron revealed its highly crystalline nature.

To investigate the effect of the incubating time on the morphology of $BaWO_4$ products, we used different incubating times of 10 min, 1 h, 3 h, and 6 h. As evident in Figure 4(a), irregular $BaWO_4$ products were obtained for the incubating time of 10 min. This indicates that 10 min was not enough time for the crystal growth of $BaWO_4$ products with its own morphology. As the incubating time was increased to 1 h, the regularity of the morphology of $BaWO_4$ products improved. When the incubating time was further increased to 3 h and 6 h, a highly improved morphology of $BaWO_4$ products was obtained. Therefore, the incubating time of 3 h was shown to be an efficient time for the formation of good morphology of $BaWO_4$ products with its own morphology. It should be noted that the size and morphology did not change when the incubating time was increased above 1 h.

Figure 5 shows the SEM images of the $BaWO_4$ particles obtained by the microemulsion method at various molar ratios of $[Ba^{2+}]$ to $[WO_4^{2-}]$. When $[Ba^{2+}]/[WO_4^{2-}] = 0.20$, the $BaWO_4$ products showed spherical particles of 100 nm diameter, as shown in Figure 5(a). For the case of $[Ba^{2+}]/[WO_4^{2-}] = 0.50$, the $BaWO_4$ products displayed oval shapes. The average lengths of the longer axes and shorter axes were 500 nm and 200 nm, respectively. When the net inorganic surface charge was negative ($[Ba^{2+}]/[WO_4^{2-}] < 1$), the initially formed particles of $BaWO_4$ had a negative charge due to the excess WO_4^{2-} ions. These particles strongly interacted with cationic surfactants and played an important role in the morphology of $BaWO_4$ products. However, a $BaWO_4$ octahedron was observed when the molar ratio of $[Ba^{2+}]$ to $[WO_4^{2-}]$ was equal to 1.0, as shown in Figure 5(c). When $[Ba^{2+}]$ to $[WO_4^{2-}]$ was larger than 1.0, a slightly truncated octahedron was observed, as shown in Figures 5(d) and 5(e). The sizes of the truncated octahedra were slightly larger than

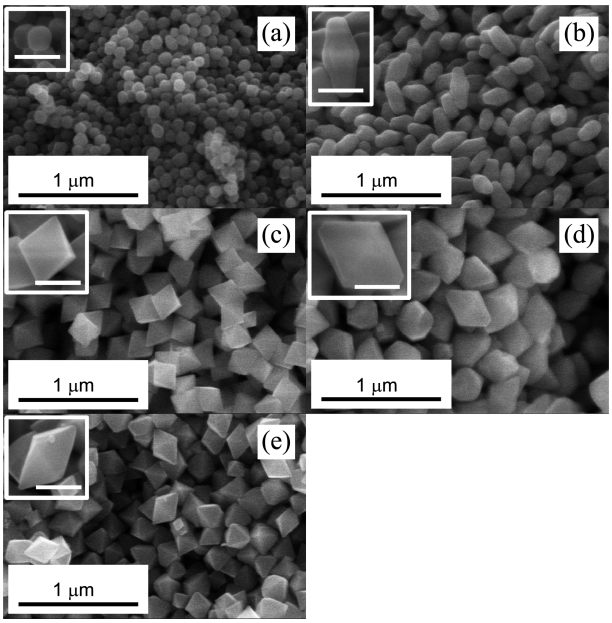

Figure 5. SEM images of $BaWO_4$ products prepared by the microemulsion method of ω = 10 at 60 °C for 3 h with different molar ratios of $[Ba^{2+}]$ to $[WO_4^{2-}]$: (a) 0.20, (b) 0.50, (c) 1.0, (d) 2.0, and (e) 5.0. The insets show high-magnification SEM images with scale bars of 200 nm.

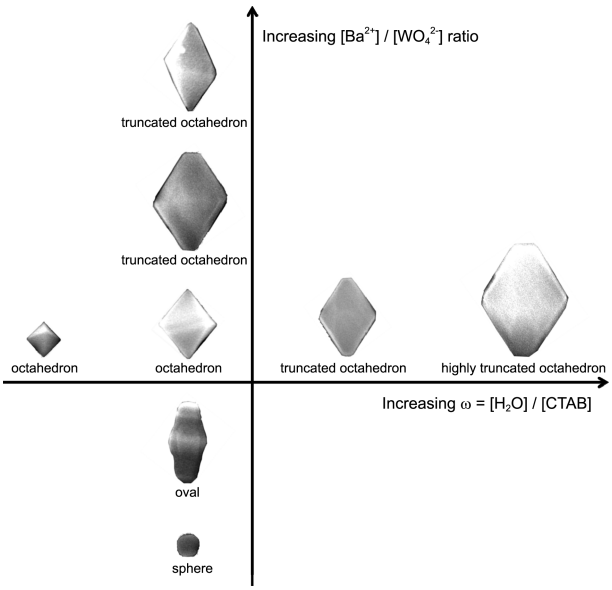

Figure 6. Schematic diagram for the morphology changes of $BaWO_4$ products with the value of ω and the molar ratios of $[Ba^{2+}]$ to $[WO_4^{2-}]$.

that of the octahedron at $[Ba^{2+}]$ to $[WO_4^{2-}]$ equal to 1.0. Because we used CTAB as a cationic surfactant, the excess Ba^{2+} ions did not significantly affect the morphology of $BaWO_4$ products. Figure 6 outlines the morphology changes of $BaWO_4$ products depending on the value of ω and the molar ratios of $[Ba^{2+}]$ to $[WO_4^{2-}]$.

In conclusion, we prepared sub-micron sized $BaWO_4$ octahedra by using the microemulsion method with the CTAB/water/cyclohexane/*n*-butanol quaternary system. The value of ω (= $[H_2O]$/[CTAB]) and the molar ratios of $[Ba^{2+}]$ to $[WO_4^{2-}]$ played an important role in the control of morphology of $BaWO_4$ products. As the value of ω increased, the size of the octahedron also increased. The degree of truncation of octahedra increased with the value of ω above 14. When the molar ratios of $[Ba^{2+}]$ to $[WO_4^{2-}]$ was less than 1.0, the morphology of $BaWO_4$ products were strongly affected by the molar ratios of $[Ba^{2+}]$ to $[WO_4^{2-}]$. However, excess Ba^{2+} did not significantly affect the morphology of $BaWO_4$ octahedra at the molar ratios of $[Ba^{2+}]$ to $[WO_4^{2-}]$ larger than 1.0,

Experimental Section

$Ba(NO_3)_2$ (99%, Sigma Aldrich), $Na_2WO_4{\cdot}2H_2O$ (99%, Sigma Aldrich), cetyltrimethyl ammonium bromide (98%, CTAB, TCI), cyclohexane (99%, Sigma Aldrich), and *n*-butanol (99%, Sigma Aldrich) were used as received without any further purification. A microemulsion method was employed using the CTAB/water/cyclohexane/*n*-butanol quaternary system. For the preparation of the transparent microemulsion solution of $Ba(NO_3)_2$, 2 mL of 0.1 M $Ba(NO_3)_2$ aqueous solution was added to a solution containing 4.0 g of CTAB, 40 mL of cyclohexane, and 8 mL of *n*-butanol. The mixed solution was stirred for 10 min to form the transparent microlemulsion. A $Na_2WO_4{\cdot}2H_2O$ microemulsion solution was also prepared with 2 mL of 0.1 M $Na_2WO_4{\cdot}2H_2O$ aqueous solution, while keeping the other conditions the same. In a typical preparation of $BaWO_4$ products, these two transparent emulsion solutions were mixed together and then heated to 60 in a water bath for 3 h. The products were centrifuged and washed with ethanol and acetone several times. Finally, the products were collected and dried at 60 °C.

To investigate the morphology dependence on the molar ratio (ω) of $[H_2O]$ to [CTAB], we used different amounts of CTAB while keeping the other conditions unchanged. To investigate the morphology dependence on the reaction times, various incubating times (10 min, 1 h, 3 h, and 6 h) were used. We also used different molar ratios of $[Ba^{2+}]$ to $[WO_4^{2-}]$ by changing the concentration of $Na_2WO_4{\cdot}2H_2O$ while fixing the concentration of the $Ba(NO_3)_2$ solution at 0.1 M. The crystal structures of the $BaWO_4$ products were analyzed through power X-ray diffraction (XRD, PANalytical, X'PERT PRO MPD) with Cu Kα radiation. The morphologies of the $BaWO_4$ products were characterized using scanning electron microscopy (SEM, Hitachi S-4300) and high resolution transmission electron microscopy (HRTEM, JEOL JEM-3010).

Acknowledgments. This study was supported by the research fund of Dankook University in 2012.

References

1. Zhang, Y.; Deng, B.; Zhang, T.; Gao, D.; Xu, A. W. *J. Phys. Chem. C* **2010**, *114*, 5073.

2. Huang, M. H.; Lin, P. H. *Adv. Funct. Mater.* **2012**, *22*, 14.
3. Antonietti, M.; Ozin, G. A. *Chem. Eur. J.* **2004**, *10*, 28.
4. Mann, S. *Angew. Chem. Int. Ed.* **2000**, *39*, 3392.
5. Tojo, C.; Blanco, M. C.; Rivadulla, F.; López-Quintela, M. A. *Langmuir* **1997**, *13*, 1970.
6. Debuigne, F.; Jeunieau, L.; Wiame, M.; Nagy, J. B. *Langmuir* **2000**, *16*, 7605.
7. Cölfen, H.; Mann, S. *Angew. Chem. Int. Ed.* **2003**, *42*, 2350.
8. Xia, Y.; Xiong, Y.; Lim, B.; Skrabalak, S. E. *Angew. Chem. Int. Ed.* **2009**, *48*, 60.
9. Chen, J.; Lim, B.; Lee, E. P.; Xia, Y. *Nano Today* **2009**, *4*, 81.
10. Park, J.; An, K.; Hwang, Y.; Park, J. G.; Noh, H. J.; Kim, J. Y.; Park, J. H.; Hwang, N. M.; Hyeon, T. *Nat. Mater.* **2004**, *3*, 891.
11. Kuo, C. H.; Huang, M. H. *J. Phys. Chem. C* **2008**, *112*, 18355.
12. Xu, H.; Wang, W.; Zhu, W. *J. Phys. Chem. B* **2006**, *110*, 13829.
13. Shi, H.; Qi, L.; Ma, J.; Cheng, H. *J. Am. Chem. Soc.* **2003**, *125*, 3450.
14. Kwan, S.; Kim, F.; Akana, J.; Yang, P. *Chem. Commun.* **2001**, 447.
15. Luo, Y.; Tu, Y.; Yu, B.; Liu, J.; Li, J.; Jia, Z. *Mater. Lett.* **2007**, *61*, 5250.
16. Shi, H.; Qi, L.; Ma, J.; Cheng, H. *Chem. Commun.* **2002**, 1704.
17. Liu, Y.; Chu, Y. *Mater. Chem. Phys.* **2005**, *92*, 59.